

THE EFFECT OF COUPLE-STRESSES ON STRESS CONCENTRATION AROUND A RIGID CIRCULAR INCLUSION IN A HALF-PLANE UNDER TENSION

S. ITOU (HACHINOHE)

The two-dimensional linearised theory of couple-stress elasticity has been applied to investigate the stress distribution in a half-plane having a perfectly rigid circular inclusion. Simple tension acts in parallel to the plane boundary. The solution is illustrated by some numerical results.

1. INTRODUCTION

The couple-stress solution for uniformly loaded plate containing a circular hole has been investigated by MINDLIN [1]. A considerable decrease of the stress concentration factor is observed. In contrast to the solution, the couple stresses lead to an increase of the stress concentration in the case of a rigid circular inclusion [2]. Recently, SHIRIAEV has verified the above results experimentally using the photoelastic method [3, 4].

In the present paper, a theoretical solution is given for the stresses in an elastic Cosserat half-plane having a rigid circular inclusion under tension. The Schmidt method is used to solve the problem because the bipolar coordinate system can not be used [5]. The numerical calculations are carried out to clarify the effect of the couple stresses on stress concentration.

2. FORMULATION

A polar coordinate system r, θ and rectangular Cartesian coordinates x, y are chosen in the plane perpendicular to the axis of the cylindrical rigid inclusion of radius a as shown in Fig. 1. The relation between the two systems of coordinates is

$$(2.1) \quad x = r \sin \theta, \quad y = r \cos \theta.$$

The semi-space is bounded by the plane boundary $y=b$ and the center of the inclusion is at the origin. Far from the inclusion, a uniform tensile stress P acts parallel to the x -axis. The problem is considered in a state of plane strain without body forces and body couples. The fundamental equations are given in reference [1]. The boundary conditions of the present problem are

i) at infinity $x=\pm\infty$,

$$(2.2) \quad \sigma_x = P, \quad \sigma_y = \tau_{xy} = \tau_{yx} = \mu_x = \mu_y = 0,$$

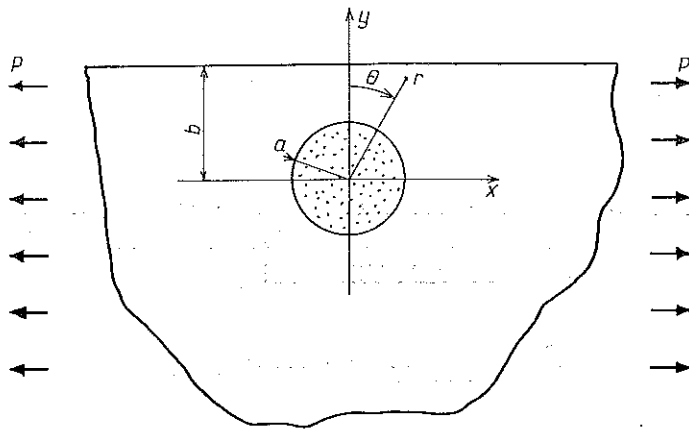


Fig. 1. Coordinate system.

ii) along the plane edge $y=b$,

$$(2.3) \quad \sigma_y = \tau_{yx} = \mu_y = 0,$$

iii) and along the contacting surface $r=a$,

$$(2.4) \quad u_r = u_\theta = \omega_z = 0.$$

Then the Airy stress function ϕ and the couple-stress function ψ have the forms

$$(2.5) \quad \begin{aligned} \phi &= \frac{P}{4} r^2 \{1 + \cos(2\theta)\} - D_1 \log r + \sum_{n=1}^{\infty} \{D_{n+1}/r^n + E_n/r^{n-2}\} \cos(n\theta) + \\ &\quad + 1/(2\pi) \int_{-\infty}^{\infty} (A + By) e^{i\xi|y-t\zeta x|} d\xi, \\ \psi &= \sum_{n=1}^{\infty} \{F_n/r^n + G_n K_n(r/l)\} \sin(n\theta) + 1/(2\pi) \int_{-\infty}^{\infty} \{A_1 e^{i\xi|y|} + c_1 e^{ky} + c_1 e^{-ix}\} d\xi, \end{aligned}$$

where $k = (\xi^2 l^2 + 1)^{1/2}/l$, l is the new material constant, and K_n is the modified Bessel function of the second kind. From the compatibility equations A_1 and F_n are represented by B and E_n respectively,

$$(2.6) \quad \begin{aligned} A_1 &= -4(1-\nu)l^2 i\xi B, \\ F_n &= -8(1-\nu)(1-n)l^2 E_n, \end{aligned}$$

where ν is Poisson's ratio. Using Eqs. (2.5) and (2.6), we obtain the stress, displacement and rotation components. For instance, the displacement and rotation components are written as

$$(2.7) \quad \begin{aligned} 2\mu u_x &= P(1-\nu)r \sin \theta + D_1 \sin \theta/r + \sum_{n=1}^{\infty} D_{n+1} [n \sin \{(n+1)\theta\}/r^{n+1}] + \\ &\quad + \sum_{n=1}^{\infty} E_n [(n-1) \sin \{(n+1)\theta\}/r^{n-1} - 8(n-1)n(1-\nu)l^2 \sin \{(n+1)\theta\}/r^{n+1}] - \end{aligned}$$

$$\begin{aligned}
 (2.7) \quad & -(3-4\nu) \sin \{(n-1)\theta\} / r^{n-1} + \sum_{n=1}^{\infty} G_n \left[-\frac{n}{r} K_n(r/l) \cos(n\theta) \sin \theta - \right. \\
 & \left. - \{K_{n-1}(r/l) + K_{n+1}(r/l)\} \sin(n\theta) \cos \theta / (2l) \right] + \frac{1}{2\pi} \int_{-\infty}^{\infty} [Ai[\xi e^{|\xi|y}] + \\
 & + Bi[2(1-\nu)|\xi|/\xi + \xi y + 4(1-\nu)l^2\xi|\xi|]e^{|\xi|y}] + C_1[-ke^{ky}] e^{-k\xi x} d\xi + f_1(y), \\
 2\mu u_y = & -Pvr \cos \theta + D_1 \cos \theta / r + \sum_{n=1}^{\infty} D_{n+1} [n \cos \{(n+1)\theta\} / r^{n+1}] + \\
 & + \sum_{n=1}^{\infty} E_n [(n-1) \cos \{(n+1)\theta\} / r^{n-1} + (3-4\nu) \cos \{(n-1)\theta\} / r^{n-1} - \\
 & - 8(n-1)n(1-\nu)l^2 \cos \{(n+1)\theta\} / r^{n+1}] + \\
 & + \sum_{n=1}^{\infty} G_n [-nK_n(r/l) \cos(n\theta) \cos \theta / r + \{K_{n-1}(r/l) + \\
 & + K_{n+1}(r/l)\} \sin(n\theta) \sin \theta / (2l)] + \frac{1}{(2\pi)} \int_{-\infty}^{\infty} [A[-|\xi|e^{|\xi|y}] + \\
 & + B[1-2y-|\xi|y-4(1-\nu)l^2\xi^2]e^{|\xi|y}] + iC_1[-\xi e^{ky}] e^{-k\xi x} d\xi + f_2(x), \\
 (2.8) \quad 4\mu\omega_z = & \sum_{n=1}^{\infty} E_n [-8(1-\nu)(n-1) \sin(n\theta) / r^n] + \sum_{n=1}^{\infty} G_n [[n^2 K_n(r/l) / r^2 + \\
 & + \{K_{n-1}(r/l) + K_{n+1}(r/l)\} / (2rl) - \{K_{n-2}(r/l) + 2K_n(r/l) + \\
 & + K_{n+2}(r/l)\} / (4l^2)] \sin(n\theta)] + \frac{1}{(2\pi)} \int_{-\infty}^{\infty} [iB[-4(1-\nu)\xi e^{|\xi|y}] + \\
 & + C_1[-(\xi^2 - k^2)e^{ky}]] e^{-k\xi x} d\xi + f'_2(x) - f'_1(y),
 \end{aligned}$$

where μ is the shear modulus and the functions $f_1(y)$ and $f_2(x)$ are produced when we integrate the strain components. Considering the supplemental conditions

$$\begin{aligned}
 (2.9) \quad u_x &= 0 \quad \text{for } x=0, \\
 u_y &= \text{const.} \quad \text{for } x=\pm\infty \quad \text{and} \quad y=0,
 \end{aligned}$$

we obtain

$$(2.10) \quad f_1(y) = f_2(x) = 0.$$

From Eq. (2.3), the next relations are to be written by using Fourier transformation,

$$\begin{aligned}
 (2.11) \quad A &= \sum_{n=0}^{\infty} q_1^n D_{n+1} + \sum_{n=1}^{\infty} q_2^n E_n + \sum_{n=1}^{\infty} q_3^n G_n, \\
 B &= \sum_{n=0}^{\infty} q_4^n D_{n+1} + \sum_{n=1}^{\infty} q_5^n E_n + \sum_{n=1}^{\infty} q_6^n G_n, \\
 C_1 &= i \sum_{n=0}^{\infty} q_7^n D_{n+1} + i \sum_{n=1}^{\infty} q_8^n E_n + i \sum_{n=1}^{\infty} q_9^n G_n,
 \end{aligned}$$

where $q_1^n, q_2^n, \dots, q_9^n$ are omitted. Then, through Eqs. (2.5) and (2.11) we obtain the stress, displacement and rotation components which satisfy Eqs. (2.2) and (2.3). The remaining boundary conditions at the contacting surface $r=a$ give the following equations:

$$(2.12) \quad \begin{aligned} & \sum_{n=0}^{\infty} D_{n+1} R_{na}^{(1)} + \sum_{n=1}^{\infty} E_n R_{na}^{(2)} + \sum_{n=1}^{\infty} G_n R_{na}^{(3)} = -Pr (\sin^2 \theta - \nu), \\ & \sum_{n=0}^{\infty} D_{n+1} R_{na}^{(4)} + \sum_{n=1}^{\infty} E_n R_{na}^{(5)} + \sum_{n=1}^{\infty} G_n R_{na}^{(6)} = -Pr \sin \theta \cos \theta, \\ & \sum_{n=0}^{\infty} D_{n+1} R_{na}^{(7)} + \sum_{n=1}^{\infty} E_n R_{na}^{(8)} + \sum_{n=1}^{\infty} G_n R_{na}^{(9)} = 0, \end{aligned}$$

where $R_{na}^{(1)}, R_{na}^{(2)}, \dots, R_{na}^{(9)}$ are omitted. Equation (2.12) can be solved for the coefficients D_{n+1}, E_n and G_n by a modified version of the Schmidt method [6]. Once these coefficients are known, the entire stress field is completely determined.

3. NUMERICAL EXAMPLE AND RESULTS

The stresses σ_r and σ_θ at $r=a$ are computed numerically for Poisson's ratio $\nu=0.25$. It is easy to estimate the numerical integrations which occur in the present calculations because the integrands decay rapidly. The first ten terms of the infinite series are retained. The coefficients D_{n+1} , E_n and G_n are shown, as an example in the Table 1 for $a/b=0.6667$ and $l/a=0.5$. The results of σ_r/P and σ_θ/P at $r=a$ are

Table 1. Coefficients D_{n+1} , E_n and G_n for $a/b=0.6667$ and $l/a=0.5$.

	$n=1$	2	\dots	9	10
D_n	-0.10988×10^{-0}	-0.82528×10^{-2}	\dots	0.27583×10^{-5}	0.87786×10^{-6}
E_n	0.15792×10^{-1}	0.17356×10^0	\dots	-0.15976×10^{-5}	0.89578×10^{-7}
G_n	-0.34360×10^{-1}	-0.10395×10^1	\dots	0.18663×10^{-7}	-0.18076×10^{-9}

shown in Figs. 2 through 7 versus θ . In Figs. 8 and 9, the stresses σ_r/P at $r=a$ and $\theta=90^\circ$ and σ_θ/P at $r=a$ and $\theta=0^\circ$ are plotted versus l/a , respectively. The results for $a/b=0.2$ are almost coincident with those given by BANKS and SOKOLOWSKI [2]. The foregoing analysis is limited to plane-strain conditions. However, it can be shown that all of the same equations apply for generalized plane-stress conditions if the following transformations are made [7]:

$$(3.1) \quad \begin{aligned} \nu &\rightarrow \nu_\sigma/(1+\nu), \\ l &\rightarrow l_\sigma [(1+\nu_\sigma)/(1+2\nu_\sigma)]^{1/2}, \end{aligned}$$

where the quantities with a subscript σ refer to generalized plane-stress conditions. From the above results it may be remarked,

i) For the case of a rigid inclusion, the couple-stresses lead to a considerable increase of the stress concentration as pointed out by references [2, 4].

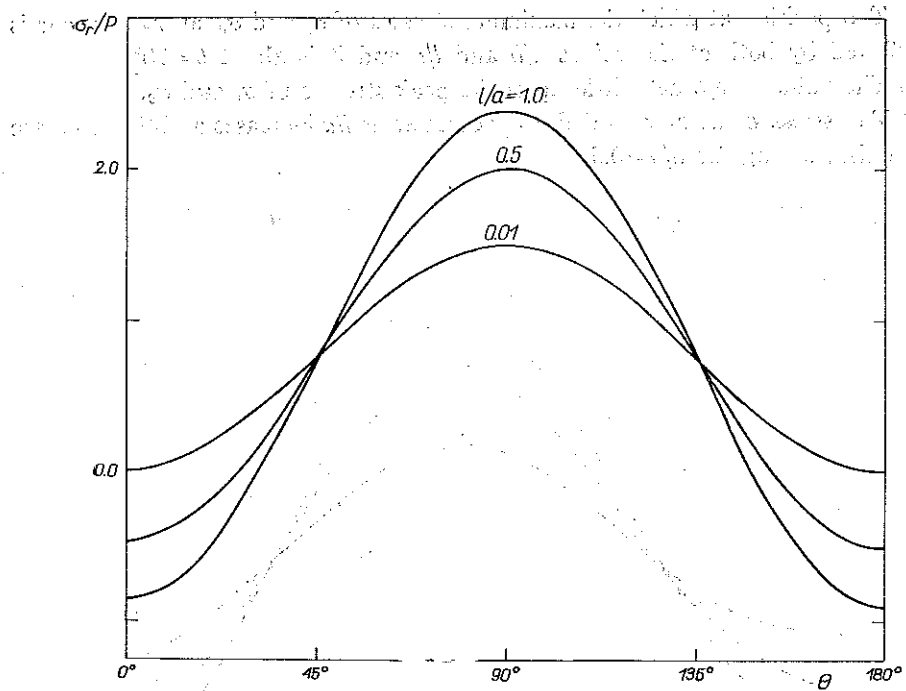


Fig. 2. σ_r/P at $r=a$ for $a/b=0.2$ versus θ .

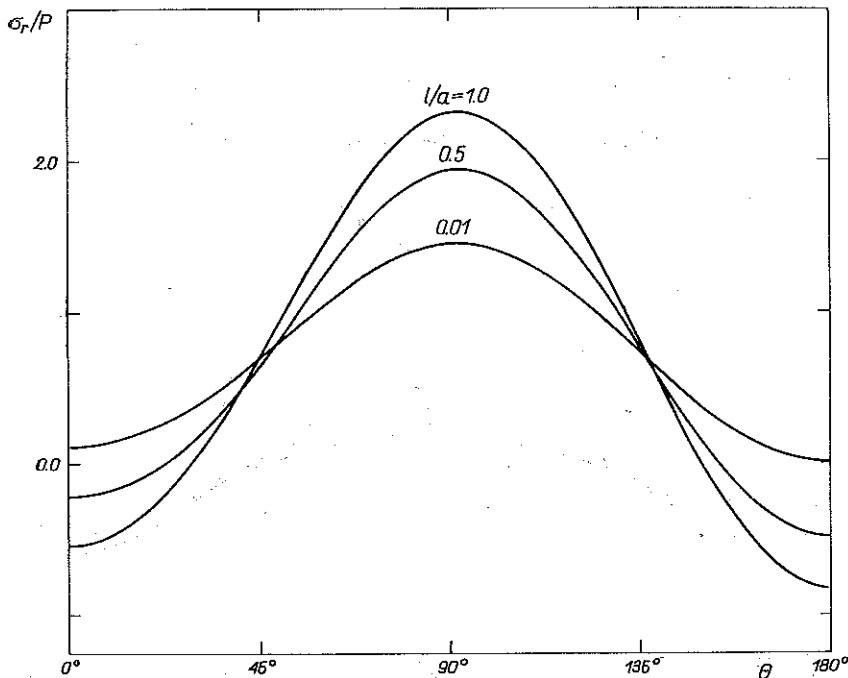


Fig. 3. σ_θ/P at $r=a$ for $a/b=0.5$ versus θ .

- ii) The position at which the maximum stresses of σ_r and σ_θ at $r=a$ occur is less affected by both of the values a/b and l/a and it is about $\theta=90^\circ$.
- iii) The value of a/b acts little upon the peak stresses of σ_r and σ_θ .
- iv) The stress σ_θ at $r=a$ and $\theta=0^\circ$ decreases as l/a increases and the decrease is somewhat strong for $a/b=0.5$.

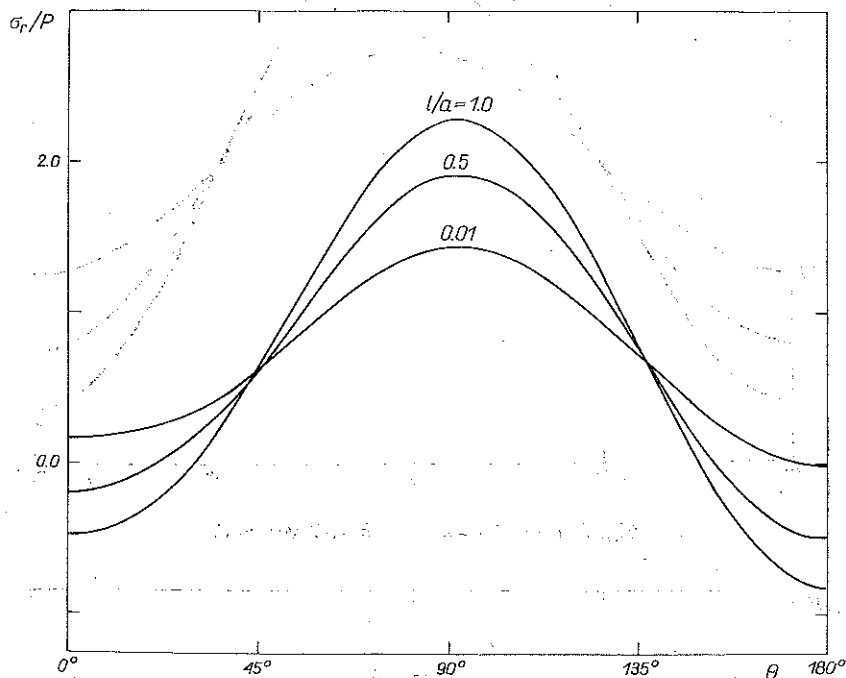


Fig. 4. σ_r/P at $r=a$ for $a/b=0.667$ versus θ .

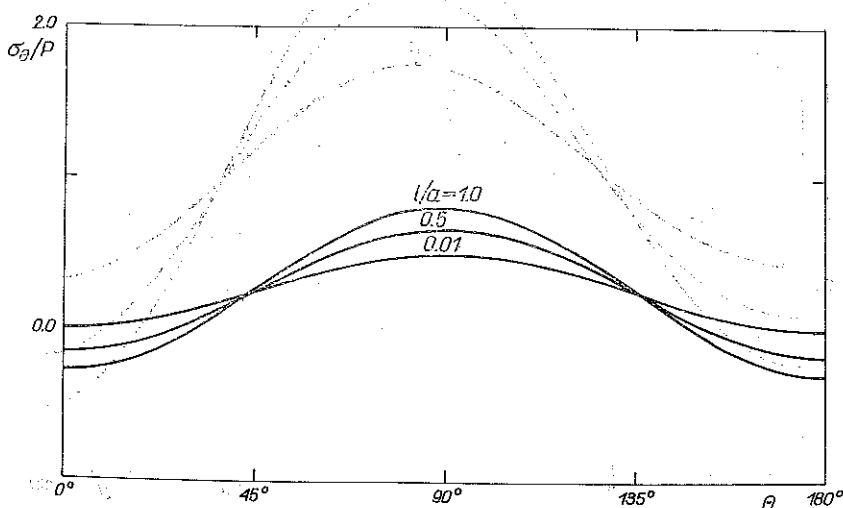


Fig. 5. σ_θ/P at $r=a$ for $a/b=0.2$ versus θ .

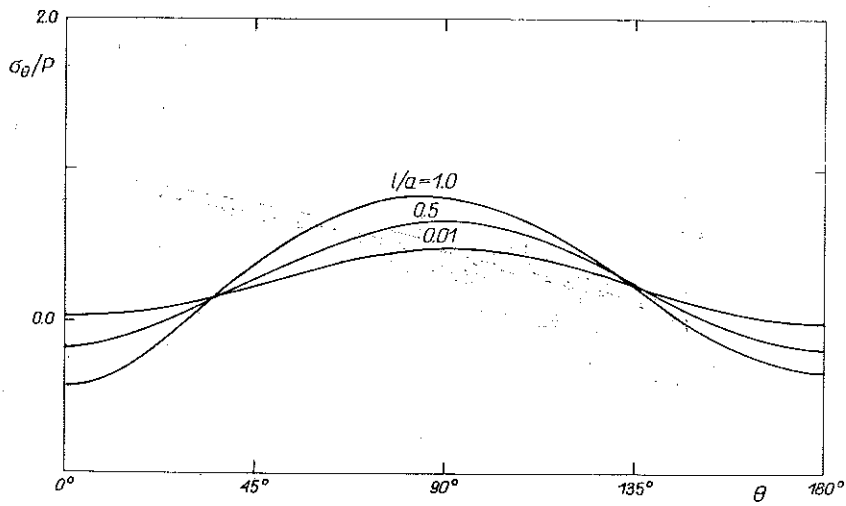


Fig. 6. σ_θ/P at $r=a$ for $a/b=0.5$ versus θ .

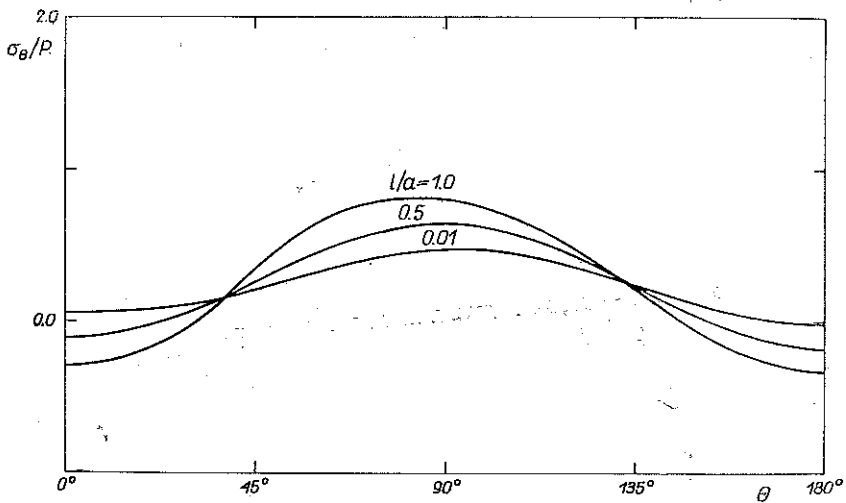


Fig. 7. σ_θ/P at $r=a$ for $a/b=0.6667$ versus θ .

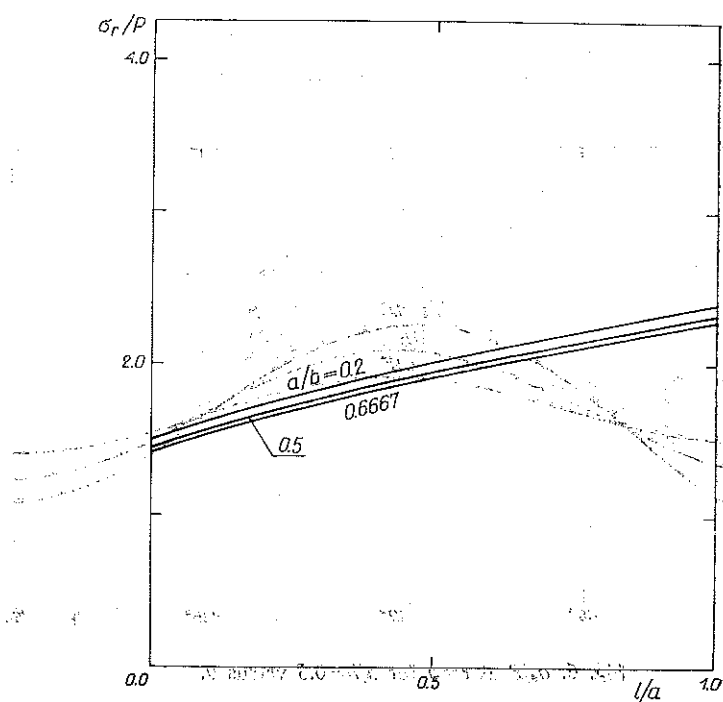


Fig. 8. σ_r/P at $r=a$ and $\theta=90^\circ$ versus l/a .

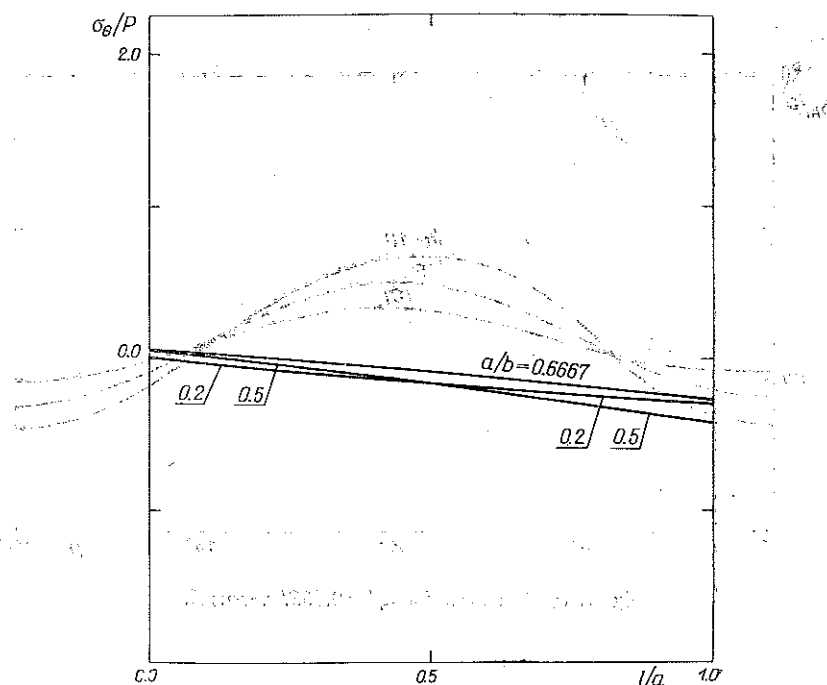


Fig. 9. σ_θ/P at $r=a$ and $\theta=0^\circ$ versus l/a .

ACKNOWLEDGMENT

The author would like to acknowledge the continual encouragement and directions of Prof. Dr. Akira ATSUMI, Tohoku University, in the preparation of this paper.

REFERENCES

1. R. D. MINDLIN, *Influence of couple-stresses on stress concentrations*, Exp. Mech., 3, 1-7, 1963.
2. C. B. BANKS and M. SOKOLOWSKI, *On certain two-dimensional applications of the couple stress theory*, Int. J. Solids Structures, 4, 15-29, 1968.
3. I. M. SHIRIAEV, *Issledowanie vlivaniia masshtabnogo faktora na koncentraciju napriazhenij okolo otverstij*, Mekh. Polim., 3, 566, 1970.
4. I. M. SHIRIAEV, *Vliyanie momentnykh napriazhenij na koncentraciju napriazhenij vblizi cylindriuekskoj neodnorodnosti v rastianutoj polose*, Izv. Vyssh. Uchebn. Zaved. Mashinostr., 8, 13-17, 1974.
5. S. ITOU, *The effect of couple-stresses on stress concentrations around a cylindrical cavity in a half-plane under tension*, Acta Mechanica [in press].
6. P. M. MORSE and H. FESHBACH, *Methods of theoretical physics I*, McGraw-Hill, 926, 1953.
7. C. W. BERT and F. J. APPL, *General solution for two-dimensional couple-stress elasticity*, AIAA Journal, 6, 968-969, 1968.

STRESZCZENIE

WPŁYW NAPREŻEŃ MOMENTOWYCH NA KONCENTRACJĘ NAPREŻEŃ WOKÓŁ SZTYWNEJ KOŁOWEJ INKLUSJI W PÓŁPRZESTRZENI PODDANEJ ROZCIĄGANIU

Do badania rozkładu napreżeń w półprzestrzeni zawierającej idealnie sztywną kołową inkluzję zastosowano zlinearyzowaną momentową teorię sprężystości. Proste rozciąganie odbywa się równolegle do płaskiego brzegu. Rozwiązanie zilustrowano na kilku przykładach liczbowych.

Резюме

ВЛИЯНИЕ МОМЕНТНЫХ НАПРЯЖЕНИЙ НА КОНЦЕНТРАЦИЮ НАПРЯЖЕНИЙ ВОКРУГ ЖЕСТКОГО КРУГОВОГО ВКЛЮЧЕНИЯ В ПОЛУПРОСТРАНСТВЕ ПОДВЕРГНУТОМ РАСТЯЖЕНИЮ

Для исследования распределения напряжений в полупространстве, содержащем идеально жесткое круговое включение, применена линеаризованная моментная теория упругости. Простое растяжение происходит параллельно плоской границе. Решение иллюстрируется на нескольких числовых примерах.

DEPARTMENT OF MECHANICAL ENGINEERING
HACHINOHE INSTITUTE OF TECHNOLOGY, HACHINOHE, JAPAN

Received August 13, 1976.